

Electrically Tunable Anomalous Hall Effect in Pt Thin Films

Sunao Shimizu,^{1,*} Kei S. Takahashi,¹ Takafumi Hatano,¹ Masashi Kawasaki,^{1,2}
Yoshinori Tokura,^{1,2} and Yoshihiro Iwasa^{1,2}

¹RIKEN Center for Emergent Matter Science, Wako, Saitama 351-0198, Japan

²Department of Applied Physics and Quantum Phase Electronics Center, University of Tokyo, Bunkyo, Tokyo 113-8656, Japan
(Received 29 May 2013; published 20 November 2013)

Pt is often considered to be an exchange-enhanced paramagnetic material, in which the Stoner criterion for ferromagnetism is nearly satisfied and, thus, external stimuli may induce unconventional magnetic characteristics. We report that a nonmagnetic perturbation in the form of a gate voltage applied via an ionic liquid induces an anomalous Hall effect (AHE) in Pt thin films, which resembles the AHE induced by the contact to Bi-doped yttrium iron garnet. Analysis of detailed temperature and magnetic field experiments indicates that the evolution of the AHE with temperature can be explained in terms of large local moments; the applied electric field induces magnetic moments as large as $\sim 10 \mu_B$ that follow the Langevin function.

DOI: [10.1103/PhysRevLett.111.216803](https://doi.org/10.1103/PhysRevLett.111.216803)

PACS numbers: 73.20.-r, 73.50.-h, 75.70.Cn

At the nanometer scale, late transition metals, e.g., Pd and Pt, have presented exotic physical properties quite different from bulk characteristics. For example, ferromagnetic behavior has been extensively reported in nanoparticles and clusters [1–5], which is considered highly important in view of potential applications for magnetic storage media [6,7]. On the other hand, it has been reported that the magnetic proximity effect can induce spin polarized electrons in Pt thin films [8,9]. In particular, reports of the magnetic proximity effect in Pt and yttrium iron garnet (YIG) heterostructures have attracted attention [8–11] because Pt is known as a spin-current detector in spin Hall effect devices [12–14].

In general, the magnetic properties of those exchange-enhanced magnetic materials have been characterized by a peculiar band structure; the density of states at the Fermi energy nearly satisfies the Stoner criterion for ferromagnetism [15–17]. This means that a relatively small modulation in electronic structures may cause incipient ferromagnetic properties to develop. The reported ferromagnetic behavior in nanoparticles and nanowires of Pt is considered to be the consequence of nanostructure-formation-induced modulation of the electronic structure [18,19].

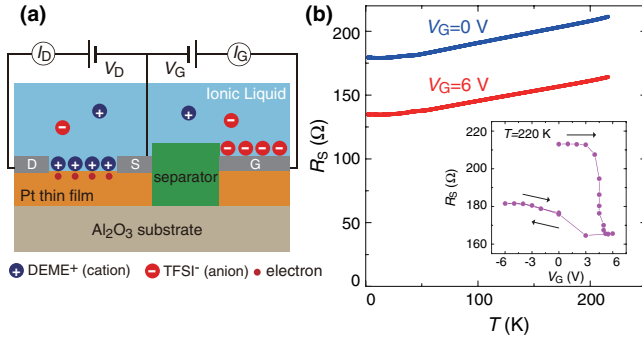
In addition to producing magnetism by nanosized engineering, tuning magnetism with an external electric field should be of significant importance for both basic sciences and potential applications. In fact, electric field tuning of magnetic properties is currently attracting a great deal of interest for low power consumption devices [20–22]. In recent years, ionic liquid gating has been used as a powerful tool to effectively control the magnetic phase [22–24]. In this case, a strong electric field is produced at the electric double layer interface between ions and electron conductors [25–28].

In this Letter, we demonstrate the gate tuning of magnetic properties in Pt thin films fabricated on Al₂O₃

substrates. The electric-double layer transistor (EDLT) configurations were employed for gating experiments. By applying positive gate biases, the sheet resistance R_S of Pt drastically decreases, and simultaneously, the anomalous Hall effect (AHE) emerges in the initially nonmagnetic Pt. Surprisingly, the AHE observed in the gated Pt thin film is quite similar to that in Pt thin films grown on Bi-doped YIG [(Bi_{0.2}Y_{0.8})₃Fe₅O₁₂, Bi:YIG] substrates. The magnetization control by nonmagnetic perturbations sheds light on the novel physical characteristics and functionalities of Pt as an exchange-enhanced magnetic material.

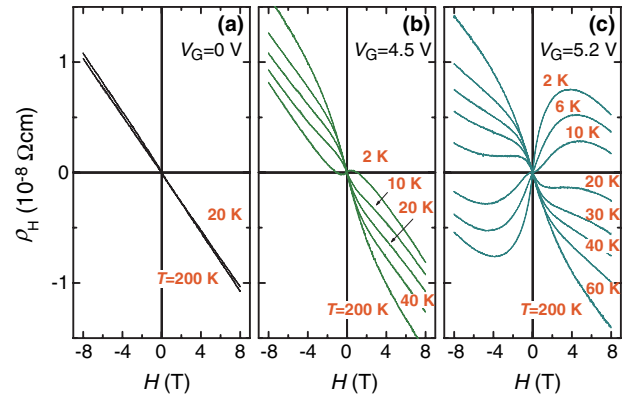
Pt thin films with a thickness of 3.2 nm were grown on an Al₂O₃ (10 $\bar{1}$ 0) plane by rf sputtering. An atomic force micrograph of the thin film is shown in the Supplemental Material [29]. For transport measurements, a Hall bar configuration with a channel size of 520 \times 30 μ m was patterned by using standard photolithography techniques. A small amount of ionic liquid *N,N*-diethyl-*N*-(2-methoxyethyl)-*N*-methylammonium bis-(trifluoromethylsulfonyl)-imide (DEME-TFSI) was deposited to cover both the channel and the gate electrode to conduct a gating experiment with a side gate configuration, as schematically shown in Fig. 1(a). A gate voltage V_G was applied and changed at $T = 220$ K, which is just above the glass transition temperature of DEME-TFSI [30,31]. The transport measurements of the Pt thin films were performed in a helium-4 refrigerator (Oxford Instruments VTI) combined with lock-in amplifiers (Stanford Research Systems SR830).

Although Pt is well known as an electrode metal in electrochemistry, few *in situ* resistance measurements in electrochemical processes have been performed [32]. The inset of Fig. 1(b) displays a drop of resistance with positive V_G . The value of R_S rapidly decreases above $V_G = 3$ V and saturates near 5.2 V. The value of R_S did not return to the initial state after the cycle of the V_G sweep, showing that the gate response is partly irreversible. Such behavior



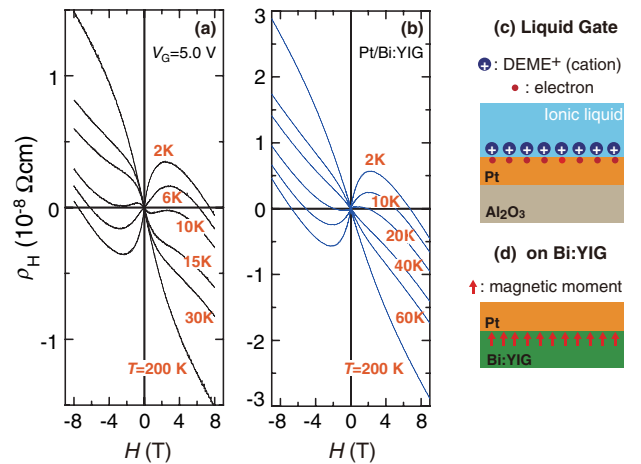
differs from the case of static charge accumulations, which have been observed in Au-EDLT [33]. In addition, the gate response appeared only when the vacuum pumping was insufficient after exposing the device to air, as discussed in the Supplemental Material [29]. Such a strong dependence on atmospheric exposure, as well as the highly nonlinear and irreversible characteristics shown in the inset of Fig. 1(b), suggests that the mechanism of resistance reduction is not a simple electrostatic one; for example, chemical processes such as hydrogen adsorption are likely involved. Temperature T dependence of R_S is shown for $V_G = 0$ V (an initial state) and 6 V in Fig. 1(b). The $R_S(T)$ curves show metallic behavior and the residual resistivity at $T = 2$ K is comparable to that reported in sputtered Pt thin films [11]. In the entire T range below 220 K, R_S decreases by nearly 20% at $V_G = 6$ V. We performed similar experiments on other Pt films with different film thicknesses as well. The gating effect decreases with increasing thickness and becomes obscure when the film is thicker than ~ 5 nm.

Figures 2(a)–2(c) show the T dependences of Hall resistivity ρ_H at (a) $V_G = 0$, 4.5 , and 5.2 V, respectively. We applied and changed V_G at $T = 220$ K, then measured the temperature dependence of ρ_H for each V_G . In the case of $V_G = 0$ V, the Hall voltage linearly depends on the magnetic field H as shown in Fig. 2(a). The Hall coefficient R_H is essentially T independent, as expected for paramagnetic metals [34]. Assuming the single band relation $R_H = 1/ne$ (e is the elementary electric charge), the nominal electron carrier density n was $\sim 5 \times 10^{23} \text{ cm}^{-3}$, which is comparable to the results reported in Pt thin films on Si substrates [8]. When the resistance drop was observed at $V_G \geq 4$ V, we encountered anomalous behavior in ρ_H . The $\rho_H(H)$ relation became highly nonlinear with increasing V_G as shown in Figs. 2(b) and 2(c). As in the case of the V_G -induced resistance drop, the H dependence of ρ_H was also irreversible against V_G . Finite nonlinear Hall voltage remained when V_G was returned from $V_G = 5.2$ to 0 V. At



$T = 200$ K, we observed the downward bending of ρ_H for positive H , whereas the curvature was changed to upward bending upon cooling. One interpretation of such a nonlinear Hall curve might be a multicarrier model; however, attempts to fit the data with such a model were unsuccessful. We suggest an alternate scenario involving the AHE due to the similarity to Pt/Bi:YIG heterostructures.

Figure 3 shows a comparison of the T dependence of the Hall response in two different systems: (a) ionic liquid-gated Pt at $V_G = 5.0$ V and (b) Pt/Bi:YIG bilayer consisting of 7 nm Pt film grown on the (111) facet of Bi:YIG substrate. We performed both the upward and downward H



(a) T dependence of ρ_H at $V_G = 5.0$ V. The anomalous Hall effect was induced under the application of the gate biases. (b) T dependence of ρ_H in a Pt/Bi:YIG heterostructure. The AHE observed in Pt/Bi:YIG is due to a magnetic proximity effect [8]. The schematic pictures of the two configurations are shown in (c) for liquid-gated Pt and (d) for Pt/Bi:YIG. Both structures induce an AHE, as shown in (a) and (b), respectively.

sweep and observed no hysteresis in the $\rho_H(H)$ curves. Resemblance of these two is striking, taking the difference between the two systems into account. The schematic pictures of the two configurations are shown in Figs. 3(c) and 3(d), respectively. For the latter system, the $\rho_H(H)$ curves in Fig. 3(b) are in accord with the recent report by Huang *et al.* [8], where the nonlinear Hall resistance was attributed to the AHE induced by the contact to a ferromagnetic insulator. Huang *et al.* claimed that the magnetic moments at Fe sites in the YIG substrates induced local magnetic moments in Pt. Similarities in the Hall curves of the gated Pt and the Pt/Bi:YIG bilayer, in terms of T and H dependences, lead us to conclude that the nonlinear behavior of ρ_H in the gated Pt is also originated from the AHE. We stress that the present AHE occurs in pure Pt without any doping or contact to ferromagnetic materials.

Figure 4(a) shows the T dependence of the anomalous Hall resistivity ρ_H^A at $H = 8$ T defined as a deviation of ρ_H from the normal (Lorentz force) H -linear component. Here, we used the values of ρ_H at $V_G = 0$ V as the normal component in order to estimate ρ_H^A because the reliable estimation of the normal components is difficult in the measured H range. As seen in Fig. 4(a), ρ_H^A shows a strong T dependence; it is negative at high temperatures, changes to positive with decreasing temperature, and shows steep enhancement at low temperatures. At $T = 2$ K and 200 K, ρ_H^A versus H is plotted in Figs. 4(b) and 4(c), respectively. It is clearly seen that the AHE is tuned by gating and shows

a sign change between low and high temperatures. The sign change of AHE as a function of T has been observed in several materials (e.g., Refs. [35–38]). One such example is SrRuO₃ [35], where ρ_H changes in magnitude and sign with T . This T dependence has been interpreted in terms of a singularity in the band structure, which can be regarded as a magnetic monopole in momentum space [35]. Since there exist many singular points in the band structure of Pt [39], a T -dependent sign change in AHE and its V_G dependence can be similarly anticipated.

In the present case of our gated Pt, however, the origin of sign change in AHE seems different from the band singularity. The Hall curves in Fig. 2(c) at intermediate temperatures such as 20 K show oscillatory behavior below $H = 4$ T. This implies that the AHE in the gated Pt is composed of positive and negative components with different saturation magnetic fields. Hence, a useful model for understanding the AHE in the gated Pt is that ρ_H consists of three components: the ordinary Hall resistivity ρ_H^0 , a positive component ρ_H^{A+} of the AHE, and a negative component ρ_H^{A-} of the AHE. In this model, ρ_H is written as

$$\rho_H = \rho_H^0 + \rho_H^A = \rho_H^0 + \rho_H^{A+} + \rho_H^{A-}. \quad (1)$$

First, we consider the positive component ρ_H^{A+} of anomalous Hall resistivity. As shown in Fig. 4(a), ρ_H^A increases with decreasing T for all V_G values. This evolution of ρ_H^A upon cooling recalls the Curie-like T dependence of

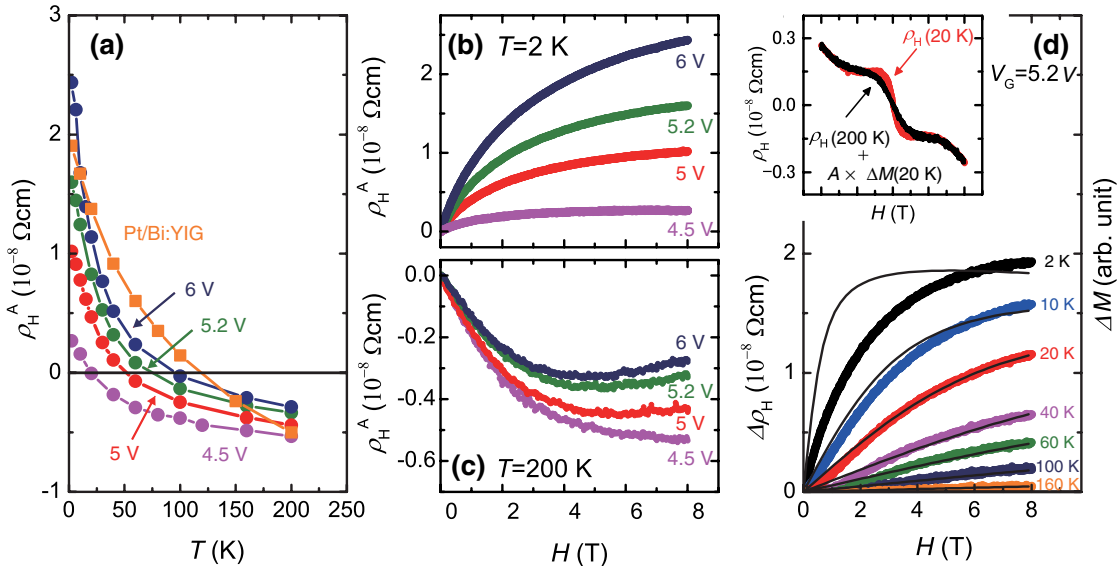


FIG. 4 (color online). (a) T dependence of anomalous Hall resistivity ρ_H^A at $H = 8$ T for various V_G values. The solid lines are guides to the eye. With decreasing temperature, ρ_H^A changes sign from negative to positive values. This behavior in Pt/Al₂O₃ is similar to that in Pt/Bi:YIG, which is also plotted. At $T = 2$ and 200 K, ρ_H^A versus H is plotted in (b) and (c), respectively. It is clearly seen that the AHE is tuned by gating and shows a sign change between low and high temperatures. (d) Magnetic field dependence of $\Delta\rho_H(T)$ for $V_G = 5.2$ V at various temperatures. The solid lines are simulations of magnetization ΔM . In the inset of (d), we compare $\rho_H(20\text{ K})$ and $\rho_H(200\text{ K}) + A \times \Delta M(20\text{ K})$, which shows that the three component model [Eq. (1)] is valid. The small deviation at low H regions likely comes from the T dependent part of ρ_H^{A-} , which was neglected in our analysis. See text for definitions of $\Delta\rho_H(T)$, ΔM , A , and ρ_H^{A-} .

magnetization. In other words, we hypothesize that the positive component ρ_H^{A+} plays a main role in the T dependence of ρ_H^A , while the negative component ρ_H^{A-} is nearly T independent. We then plot the T dependence of $\Delta\rho_H$ as a function of H for $V_G = 5.2$ V in Fig. 4(d). Here, we define $\Delta\rho_H(T) = \rho_H(T) - \rho_H(200\text{ K}) \sim \rho_H^{A+}(T) - \rho_H^{A+}(200\text{ K})$, assuming that ρ_H^{A-} is T independent. The closed circles represent the experimental data, and the solid lines represent simulations of magnetization M . In the simulation, we used the Langevin function,

$$\begin{aligned} M(T) &= NmL(mH/k_B T) \\ &= Nm[\coth(mH/k_B T) - kT/mH], \end{aligned} \quad (2)$$

where N is the number of the magnetic moments per unit volume, m is the size of the magnetic moments, and $L(x)$ is the Langevin function. In Fig. 4(d), $\Delta M(T) = M(T) - M(200\text{ K})$ is plotted. To reproduce the experimental data by simulations, m is set to be $10\ \mu_B$ and N is fixed to a constant value in all temperature ranges [we only consider the relative magnitude of $\Delta M(T)$]. As seen in Fig. 4(d), the T and H dependences of $\Delta\rho_H(T)$ are well explained by $\Delta M(T)$ except for the data at the lowest temperature (2 K). Such a discrepancy may arise when interactions between induced magnetic moments become apparent at low temperatures. This interaction was neglected in the analysis with Eq. (2). In the inset of Fig. 4(d), we compare $\rho_H(20\text{ K})$ and $\rho_H(200\text{ K}) + A \times \Delta M(20\text{ K})$, where A is the proportionality constant between $\Delta\rho_H(T)$ and $\Delta M(T)$. The comparison shows that the three component model [Eq. (1)] satisfactorily explains the data. The small deviation at low H regions probably comes from the T dependent part of ρ_H^{A-} , which was neglected in our analysis. Here, note that the size of m is not changed even in the simulations for V_G values other than 5.2 V; the number of the magnetic moments per unit volume, N , is varied to simulate the data. See Sec. S3 in the Supplemental Material [29] for detail.

The qualitative agreement between $\Delta\rho_H(T)$ and $\Delta M(T)$ provides evidence that the observed ρ_H indeed stems from the AHE in a paramagnet with local magnetic moments, as large as $10\ \mu_B$. It has been known that not only uniform long-range magnetic order but also local magnetic moments can contribute to the AHE [40,41]. For example, superparamagnetic moments have been reported to induce the AHE in Co-doped TiO_2 [40] and Pt thin films embedded with Fe nanoparticles [41]. The magnetoresistance effect for the gated Pt also supports the appearance of the magnetic moments, as mentioned in Sec. S4 in the Supplemental Material [29]. The mechanism of the induced local moments in the gated Pt film remains the subject of ongoing investigation. A conceivable scenario is that chemisorbed species on the Pt channel induce ferromagnetism in a manner similar to the case of nanostructures of Pt and thiol-capped thin films of Au [42,43]. Adsorbed external species such as hydrogen in the ionic

liquid may cause local electric fields at the interface of Pt, which might induce local magnetic moments in Pt with the help of its large spin-orbit interaction. Also, possible structural disorder in the Pt film would prohibit long range order of ferromagnetism, resulting in large local moments as observed in superparamagnetic systems. As a candidate of such chemisorbed species, we cannot, at this stage, completely rule out the existence of magnetic ions that accidentally contaminated the ionic liquid. Although we conducted the device fabrication and the experiments with great care, an extremely minor amount of impurity contaminations might be possible. Further investigation of the possible source of the induced magnetism in the gated Pt thin films is needed.

Finally, we comment on the negative component ρ_H^{A-} of anomalous Hall resistivity. As discussed above, ρ_H^{A-} seems nearly T independent in contrast to the highly T -dependent behavior of ρ_H^{A+} . The values of ρ_H^{A+} are negligible at $T = 200\text{ K}$, so that ρ_H^A at $T = 200\text{ K}$ in Fig. 4(c) is dominated by the negative component ρ_H^{A-} . By changing V_G from 4.5 to 6 V, $|\rho_H^A|$ slightly decreases. The origin of ρ_H^{A-} , including the V_G dependence, is left to be understood for a future work.

In summary, we have demonstrated voltage tuning of the AHE in Pt thin films in an EDLT configuration composed of completely nonmagnetic materials. The AHE was interpreted as the composition of the T dependent positive and T independent negative components. The former can be explained by large local moments as observed in superparamagnetic systems, whereas the latter remains to be understood. The T dependence of AHE in gated Pt with a sign change resembles that in Pt/Bi:YIG bilayer structures, indicating a common underlying mechanism. Thus, the voltage tuning of the AHE in paramagnetic metal Pt has further revealed a novel aspect of electronic and magnetic properties of Pt thin films.

We are grateful to J.G. Checkelsky, Y. Kozuka, Y. Ogimoto, and A. Tsukazaki for their fruitful discussions. This work was supported by Strategic International Collaborative Research Program (SICORP), Japan Science and Technology Agency (JST), JPSP Grant-in-Aid for Scientific Research (S) (Grants No. 21224009, and No. 24226002), JSPS Grant-in-Aid for Specially Promoted Research (Grant No. 25000003), and the Funding Program for World-Leading Innovative R&D on Science and Technology (FIRST Program) from JSPS. S.S. and T.H. were supported by RIKEN through the Incentive Research Grant.

*sshimizu@riken.jp

- [1] H. Hori, T. Teranishi, Y. Nakae, Y. Seino, M. Miyake, and S. Yamada, *Phys. Lett. A* **263**, 406 (1999).
- [2] B. Sampedro, P. Crespo, A. Hernando, R. Litrán, J.C. Sánchez López, C. López Cartes, A. Fernandez,

- J. Ramírez, J. González Calbet, and M. Vallet, *Phys. Rev. Lett.* **91**, 237203 (2003).
- [3] Y. Yamamoto, T. Miura, Y. Nakae, T. Teranishi, M. Miyake, and H. Hori, *Physica (Amsterdam)* **329-333**, 1183 (2003).
- [4] X. Liu, M. Bauer, H. Bertagnolli, E. Roduner, J. van Slageren, and F. Phillipp, *Phys. Rev. Lett.* **97**, 253401 (2006).
- [5] Y. Sakamoto, Y. Oba, H. Maki, M. Suda, Y. Einaga, T. Sato, M. Mizumaki, N. Kawamura, and M. Suzuki, *Phys. Rev. B* **83**, 104420 (2011).
- [6] G. Reiss and A. Hütten, *Nat. Mater.* **4**, 725 (2005).
- [7] A.-H. Lu, E. L. Salabas, and F. Schüth, *Angew. Chem., Int. Ed. Engl.* **46**, 1222 (2007).
- [8] S. Y. Huang, X. Fan, D. Qu, Y. P. Chen, W. G. Wang, J. Wu, T. Y. Chen, J. Q. Xiao, and C. L. Chien, *Phys. Rev. Lett.* **109**, 107204 (2012).
- [9] S. Geprägs, S. Meyer, S. Altmannshofer, M. Opel, F. Wilhelm, A. Rogalev, F. Gross, and S. T. B. Goennenwein, *Appl. Phys. Lett.* **101**, 262407 (2012).
- [10] S. M. Rezende, R. L. Rodríguez-Suárez, M. M. Soares, L. H. vilela-Leão, D. L. Domínguez, and A. Azevedo, *Appl. Phys. Lett.* **102**, 012402 (2013).
- [11] Y. M. Lu, Y. Choi, C. M. Ortega, X. M. Cheng, J. W. Cai, S. Y. Huang, L. Sun, and C. L. Chien, *Phys. Rev. Lett.* **110**, 147207 (2013).
- [12] Y. Kajiwara, K. Harii, S. Takahashi, J. Ohe, K. Uchida, M. Mizuguchi, H. Umezawa, H. Kawai, K. Ando, K. Takahashi, S. Maekawa, and E. Saitoh, *Nature (London)* **464**, 262 (2010).
- [13] T. Kikkawa, K. Uchida, Y. Shiomi, Z. Qiu, D. Hou, D. Tian, H. Nakayama, X.-F. Jin, and E. Saitoh, *Phys. Rev. Lett.* **110**, 067207 (2013).
- [14] H. Nakayama, M. Althammer, Y.-T. Chen, K. Uchida, Y. Kajiwara, D. Kikuchi, T. Ohtani, S. Geprägs, M. Opel, S. Takahashi, R. Gross, G. E. W. Bauer, S. T. B. Goennenwein, and E. Saitoh, *Phys. Rev. Lett.* **110**, 206601 (2013).
- [15] A. H. MacDonald, J. M. Daams, S. H. Vosko, and D. D. Koelling, *Phys. Rev. B* **23**, 6377 (1981).
- [16] V. L. Moruzzi and P. M. Marcus, *Phys. Rev. B* **39**, 471 (1989).
- [17] H. Chen, N. E. Brener, and J. Callaway, *Phys. Rev. B* **40**, 1443 (1989).
- [18] A. Delin and E. Tosatti, *Phys. Rev. B* **68**, 144434 (2003).
- [19] E. P. Lee, Z. Peng, D. M. Cate, H. Yang, C. T. Campbell, and Y. Xiz, *J. Am. Chem. Soc.* **129**, 10634 (2007).
- [20] T. Maruyama, Y. Shiota, T. Nozaki, K. Ohta, N. Toda, M. Mizuguchi, A. A. Tulapurkar, T. Shimjo, M. Shiraishi, S. Mizukami, Y. Ando, and Y. Suzuki, *Nat. Nanotechnol.* **4**, 158 (2009).
- [21] D. Chiba, S. Fukami, K. Shimamura, N. Ishiwata, K. Kobayashi, and T. Ono, *Nat. Mater.* **10**, 853 (2011).
- [22] Y. Yamada, K. Ueno, T. Fukumura, H. T. Yuan, H. Shimotani, Y. Iwasa, L. Gu, S. Tsukimoto, Y. Ikuhara, and M. Kawasaki, *Science* **332**, 1065 (2011).
- [23] M. Weisheit, S. Fähler, A. Marty, Y. Souche, C. Poinsignon, and D. Givord, *Science* **315**, 349 (2007).
- [24] K. Shimamura, D. Chiba, S. Ono, S. Fukami, N. Ishiwata, M. Kawaguchi, K. Kobayashi, and T. Ono, *Appl. Phys. Lett.* **100**, 122402 (2012).
- [25] H. Shimotani, H. Asanuma, A. Tsukazaki, A. Ohtomo, M. Kawasaki, and Y. Iwasa, *Appl. Phys. Lett.* **91**, 082106 (2007).
- [26] K. Ueno, S. Nakamura, H. Shimotani, A. Ohtomo, N. Kimura, T. Nojima, H. Aoki, Y. Iwasa, and M. Kawasaki, *Nat. Mater.* **7**, 855 (2008).
- [27] J. T. Ye, S. Inoue, K. Kobayashi, Y. Kasahara, H. T. Yuan, H. Shimotani, and Y. Iwasa, *Nat. Mater.* **9**, 125 (2010).
- [28] D. Daghero, F. Paolucci, A. Sola, M. Tortello, G. A. Ummarino, M. Agosto, R. S. Gonnelli, J. R. Nair, and C. Gerbaldi, *Phys. Rev. Lett.* **108**, 066807 (2012).
- [29] See Supplemental Material at <http://link.aps.org/supplemental/10.1103/PhysRevLett.111.216803> for device characterizations and additional experimental data.
- [30] T. Sato, G. Masuda, and K. Takagi, *Electrochim. Acta* **49**, 3603 (2004).
- [31] H. T. Yuan, H. Shimotani, A. Tsukazaki, A. Ohtomo, M. Kawasaki, and Y. Iwasa, *Adv. Funct. Mater.* **19**, 1046 (2009).
- [32] M. Sagmeister, U. Brossmann, S. Landgraf, and R. Wurschum, *Phys. Rev. Lett.* **96**, 156601 (2006).
- [33] H. Nakayama, J. T. Ye, T. Ohtani, Y. Fujikawa, K. Ando, Y. Iwasa, and E. Saitoh, *Appl. Phys. Express* **5**, 023002 (2012).
- [34] C. L. Chien and C. R. Westgate, *The Hall Effect and Its Applications* (Plenum, New York, 1979).
- [35] Z. Fang, N. Nagaosa, K. S. Takahashi, A. Asamitsu, R. Mathieu, T. Ogasawara, H. Yamada, M. Kawasaki, Y. Tokura, and K. Terakura, *Science* **302**, 92 (2003).
- [36] W.-L. Lee, S. Tatauchi, V. L. Miller, R. J. Cava, and N. P. Ong, *Science* **303**, 1647 (2004).
- [37] K. S. Takahashi, M. Onoda, M. Kawasaki, N. Nagaosa, and Y. Tokura, *Phys. Rev. Lett.* **103**, 057204 (2009).
- [38] T. Golod, A. Rydh, P. Svedlindh, and V. M. Krasnov, *Phys. Rev. B* **87**, 104407 (2013).
- [39] G. Y. Guo, S. Murakami, T.-W. Chen, and N. Nagaosa, *Phys. Rev. Lett.* **100**, 096401 (2008).
- [40] S. R. Shinde, S. B. Ogale, J. S. Higgins, H. Zheng, A. J. Millis, V. N. Kulkarni, R. Ramesh, R. L. Greene, and T. Venkatesan, *Phys. Rev. Lett.* **92**, 166601 (2004).
- [41] V. T. Volkov, V. I. Levashov, V. N. Matveev, and V. A. Berezin, *Appl. Phys. Lett.* **91**, 262511 (2007).
- [42] I. Carmeli, G. Leitius, R. Naaman, S. Reich, and Z. Vager, *J. Chem. Phys.* **118**, 10372 (2003).
- [43] A. Hernando, P. Crespo, M. A. García, E. Fernandez Pinel, J. de la Venta, A. Fernández, and S. Penadés, *Phys. Rev. B* **74**, 052403 (2006).